Shining new light on sensory brain activation and physiological measurement in seals using wearable optical technology

J. Chris McKnight
Alexander Ruesch
Kimberley Bennett
Mathijs Bronkhorst
Steve Balfour
Simon E. W. Moss
Ryan Milne
Peter L. Tyack
Jana M. Kainerstorfer
Gordon D. Hastie

This is the Author Accepted Manuscript. The final published version is available via doi:
https://doi.org/10.1098/rstb.2020.0224

McKnight, J.C., Ruesch, A., Bennett, K., Bronkhorst, M., Balfour, S., Moss, S.E.W., Milne, R., Tyack, P.L., Kainerstorfer, J.M. & Hastie, G.D. (2021) 'Shining new light on sensory brain activation and physiological measurement in seals using wearable optical technology'. *Philosophical Transactions of the Royal Society B: Biological Sciences, 376(1830).*

Shining new light on sensory brain activation and physiological measurement in seals using wearable optical technology.

J. Chris McKnight[1], Alexander Ruesch[2], Kimberley Bennett[3], Mathijs Bronkhorst[4], Steve Balfour[5], Simon E. W. Moss[1], Ryan Milne[1], Peter L. Tyack[1], Jana Kainerstorfer[2], Gordon D. Hastie[1].

Affiliations:
[1]Sea Mammal Research Unit, Scottish Oceans Institute, University of St. Andrews, St. Andrews, Scotland.
[2] Department of Biomedical Engineering, Carnegie Mellon University, 5000 Forbes Avenue, Pittsburgh, PA 15213, USA
[3] Division of Science, School of Engineering and Technology, Abertay University, Dundee, Scotland
[4]Artinis Medical Systems BV, Einsteinweg 17, 6662 PW Elst, The Netherlands.
[5]Sea Mammal Research Unit Instrumentation Group, Scottish Oceans Institute, University of St. Andrews, St. Andrews, Scotland.

Correspondence: jcm20@st-andrews.ac.uk

Keywords: fNIRS, near-infrared spectroscopy, seal, sensory ecology, brain activation

Abstract

Sensory ecology and physiology of free-ranging animals is challenging to study but underpins our understanding of decision making in the wild. Existing non-invasive human biomedical technology offers tools that could be harnessed to address these challenges. Functional near-infrared spectroscopy (fNIRS), a wearable, non-invasive biomedical imaging technique measures oxy- and deoxyhemoglobin concentration changes that can be used to detect localised neural activation in the brain. We tested the efficacy of fNIRS to detect cortical activation in grey seals (*Halichoerus grypus*) and identify regions of the cortex associated with different senses (vision, hearing and touch). Activation of specific cerebral areas in seals was detected by fNIRS in responses to light (vision), sound (hearing) and whisker stimulation (touch). Physiological parameters, including heart and breathing rate, were also extracted from the fNIRS signal, which allowed neural and physiological responses to be monitored simultaneously. This is the first time fNIRS has been used to detect cortical activation in a non-domesticated or laboratory animal. Since fNIRS is non-invasive and wearable, this study demonstrates its potential as a tool to quantitatively investigate sensory perception and brain function while simultaneously recording heart rate, tissue and arterial oxygen saturation of haemoglobin, perfusion changes and breathing rate in free-ranging animals.

1. Introduction

Animals respond continually to diverse environmental stimuli (e.g. sound, sight and touch) [1-3] to make critical ecological decisions (e.g., communication, foraging). Extensive research has described behavioural responses to such stimuli [4-7]. For example, experiments demonstrate that domestic sheep can recognize their offspring at a distance using visual and acoustic cues, with olfaction providing a final check of identity at close range before allowing suckling [8]. Specific areas of a sheep's cerebral cortex are involved in facial recognition and there is a specialized mechanism to learn offspring odours immediately after birth [9]. However, understanding how most species detect and perceive external stimuli rarely integrates information from several senses. Instead, basic knowledge of the structure [10] and function [11] of individual sensory apparatus is used along with measurements of their relative sensitivity, detection capacity, and threshold ranges [12-14]. For example, we know that deep-diving seals have acute vision adapted for the deep ocean [12], they can hear well underwater [13]; and their vibrissae can detect the wake of fish [14]; but it is currently unclear which of these senses they use at different stages of prey detection, localisation, and capture.

Although animals can perform some tasks when experimentally restricted to only one sensory system [15], and some behavioural characteristics are suggestive of task-based dominance of a particular sensory pathway (e.g. changing bearing in response to prey-derived bioluminescence [16]), under natural conditions most behaviours are based on multimodal convergence of input from several senses [3]. In addition, information from different senses may change in importance relative to other senses depending on the context. Our understanding of which senses animals rely upon to complete tasks in the wild (such as locating prey or detecting and fleeing danger) is complicated by the fact that sensing occurs in a spatially, temporally, and contextually heterogeneous environment, in which information masking and central attentional factors, such as a focus on finding prey or detecting a predator, can affect how even simple stimuli are detected and processed [17]. Given the complexity of natural environments and the dynamic interactions that free-ranging animals must process, it is important to measure sensory activation under naturalistic conditions. An ability to understand multi-sensory perception, specifically sensory cortical activation, synchronously with behaviour and physiological parameters such as heart rate, is key to understanding contextual decision-making in the wild.

Visual, auditory, mechanoreceptive, and chemoreceptive stimuli evoke responses from different regions of the cortex of the mammalian brain [18]. The location of these areas varies across mammals, but the specialization of cortical areas for different senses is shared across

mammals. If the areas of cortex activated by each sense are mapped in a species, then a method to detect activation of those regions in a free-ranging individual should identify which sense is activated during different behaviours.

Several methods are available for topographical mapping of cortical activation, but few are suitable to work with wild animals engaged in normal behaviour in their natural environments. Magnetoencephalography (MEG) and electroencephalography (EEG) can measure magnetic and electrical fields generated by neural activity with good temporal resolution, but MEG equipment is limited to the laboratory, which limits the species, contexts and environmental conditions that can be investigated. EEG signals from the brain can be overwhelmed by electrical signals from muscle tissue when animals are moving and behaving. Functional MRI (fMRI) can measure localised changes in blood oxygenation due to increases in metabolic rate of activated tissue [19]. It has excellent spatial resolution, but MRI equipment is static and laboratory-based. Alternatively, functional near-infrared spectroscopy (fNIRS) uses the same changes in haemoglobin concentration to map brain activity [20], but is non-invasive, wearable and can potentially be ruggedized to collect physiological data on animals in extreme environments [21]. Therefore, fNIRS has the potential as a tool to study animal sensory biology through brain activation in free-ranging contexts.

The haemodynamic response (HR) to stimulation is the fundamental basis by which fMRI and fNIRS identify regions of activation within the brain. In humans, the HR is characterised by an increase in [HbO] of ~1.0 μM [22] and a moderate decrease in [HbR], resulting in an increase in blood volume and blood oxygen concentration that supports increased neuronal metabolic demand in active brain regions, e.g. in the occipital cortex during a visual task. As cortical activation is proximally measured through hemodynamic and oxygenation changes, other physiological processes such as cardiac function, changes in vascular tone, respiration, and changes in blood oxygen saturation are captured by fNIRS. Heart rate, respiration, tissue-specific perfusion changes, tissue-specific oxygenation changes, arterial blood oxygenation, and blood pressure changes are all physiological signals available from raw fNIRS data [23]. While these physiological signals are generally accounted for and removed to determine the underlying cortical activation responses in neuroimaging studies, these signals are important in bioenergetics research [24] and for tracking physiological responses to environmental covariates and anthropogenic disturbance [25]. The combination of physiological and cortical activation data make fNIRS a potentially powerful tool, particularly if these measurements

could be integrated into existing behavioural and environmental data logging platforms, to measure responses to external stimuli as animals interact with their environment in the wild.

Although fNIRS has been used in a small number of terrestrial, domestic species (such as sheep and dogs) in controlled laboratory settings [26-30], it has not been used to study the sensory biology of wild animals. This method will be particularly useful for species that are accessible for attachment of a biologging device, but, once released into their natural environment, perform important behaviours where they are no longer accessible for direct observation.

Here we describe the application of fNIRS on grey seals (*Halichoerus grypus*) to map cortical activation associated with different sensory modalities. Specifically, using stimulation of three sensory modalities (vision, hearing, and mechanoreception), we describe the topographical areas of regional activation and distinction between areas associated with each sense, the shape and timing of the cerebral hemodynamic response indicative of activation, as well systemic physiological parameters collected simultaneously collected by fNIRS. Our results have significant implications for the development of biologging tools to measure sensory responses of wild animals, and their integration with physiological and behavioural metrics to allow a better understanding of reactions to complex stimuli in the wild. We propose that fNIRS has potential not only for fundamental sensory ecology research but also to study the effects of potentially distracting stimuli from human activities and harmful objects such as fishing gear, which are of growing conservation concern.

2. Materials and Methods

Ethics Statement

Procedures for capture, handling, and housing of animals conformed to the Animals (Scientific Procedures) Act 1986, under the Sea Mammal Research Units' Home Office licence (#70/7806) and were performed by personnel deemed competent under EU directive of the protection of animals used for scientific purposes.

Subject Details

Experiments were conducted with five temporarily captive juvenile grey seals (*Halichoerus grypus*) housed at the Sea Mammal Research Unit (SMRU), University of St Andrews. All animals were captured in the Moray Firth, Scotland, and transported to and temporarily housed at the SMRU animal facility; consisting of three unheated seawater pools. Animals were released to the wild following completion of the experiments.

fNIRS Instrumentation

Data were collected using a wearable near infra-red spectroscopy (NIRS) device ('Brite24' Artinis Medical Systems BV, Einsteinweg, The Netherlands) with 16 dual-wavelength emitters and eight photodiode detectors, configured to provide 20 emitter-detector pairs (channels) (Fig. 1). The 16 LED emitters each had two NIR light sources with wavelengths of 760 and 850 nm, and the eight photodiode detectors had ambient light filters. Twenty channels had an optode-detector separation distance of ~30 mm. The system contained eight short (10 mm) channels that were not included in analysis.

Fig. 1. A) visualises the optode array configuration overlayed on the head of a seal for anatomical perspective. B) visualises the anatomically and spatially accurate location of the light sources (red points) and detectors (black points) overlayed on the skull of a juvenile grey seal. Black lines indicate each of twenty 3 cm optode-detector distance channels.

Optode Attachment

A customised neoprene headcap was developed to fit the head of seals. Using three-dimensional (3D) photogrammetry software (Photomodeler Scanner 2016, Photomodeler Technologies, Vancouver, Canada), a 3D computational model of a seal head was rendered from photographs of an anesthetised juvenile grey seal and 3D-printed ('Form 2' Formlabs Inc., Somerville, MA, USA) at 1:1 scale to tailor a customised neoprene headcap that ensured contact was maintained between the seals' head and the optodes/detectors. To consistently place the optode/detectors in comparable locations across individual seals, skull features were used. The centre of the cap was placed in line with the sagittal crest, the back of the cap with the nuchal crest. The front of the cap was 2 cm caudal to the supraorbital vibrissae. Additionally, a ~10mm diameter area of fur under each optode/detector was shaved to the skin. This ensured repeatability of optode/detector location between trials and prevented fur from impeding NIR light propagation.

Determining fNIRS optode locations

To identify the anatomical position of the fNIRS emitters and detectors over the skull of a juvenile grey seal, the neoprene headcap used in experiments was fitted to the head of a freshly dead juvenile grey seal using the same cap placement described above. The headcap was then removed and a series of 40 photographs were taken of the carcass using a Nikon D90 camera and 18-70 Nikon lens with the focal length set to 18 mm. 3D photogrammetry software (Photomodeler Scanner 2016) was used to generate a 3D computational model of the seal head

that included the optode/detector locations (Model A). The tissue overlying the skull was then removed to expose the braincase. The carcass was imaged a second time (40 photographs) and a second 3D photogrammetry model was generated (Model B). Both models had a Root Mean Squared (RMS) error of < 2.0 (arbitrary units defined by Photomodeler), which is within the acceptable threshold of accuracy (RMS 0-5) recommended by Photomodeler software (De Bruyn et al 2009). Both models were exported from Photomodeler as *.stl files and combined in the software package Mesh Lab (Visual Computing Lab, Istituto di Scienza e Tecnologie dell' Informazione "A. Faedo", Italy), using anatomical features (eyes, nose, vibrissae) to align them. The optode/detector positions on the skin (Model A) were then matched to the underlying locations on the skull (Model B). The area covered by the optode/detector array is shown in Fig. 1 and was presumed to be representative of the cohort of juvenile grey seals used in experiments.

Sensory Stimuli

Visual, auditory, and tactile stimuli were selected to stimulate each sense independently. Visual stimuli consisted of the presence and absence of torchlight (50 lumens) manually shone into the eyes from a range of 30 cm. Auditory stimuli consisted of five different anthropogenic sounds (Fig. S1); these were a) pile driving (500 m), b) pile driving (40 km), c) an operational tidal turbine (low sound pressure level), d) an operational tidal turbine (high sound pressure level), and e) a training whistle. Previous research has shown that acoustic characteristics (e.g. source level, rise time, signal duration, signal frequency) can have a significant influence on the probability of detection by an animal [29]. Therefore, by selecting a range of sounds with different acoustic characteristics, we hoped to maximise the probability of inducing a haemodynamic response to the acoustic stimuli. The pile-driving signals were derived from two far-field measurements of pile driving (500m and 40km from the source) in a shallow water environment [30]. Similarly, the tidal turbine signal was generated to show comparative far-field temporal and spectral characteristics of real turbine noise [6]. The training whistle signal was a recording of a whistle used by training and husbandry personnel as a conditioned reinforcement 'bridging' signal [31] during feeding of the seals. The majority of the signals (pile driving (500 m), pile driving (40 km), the tidal turbine (low sound pressure level), and the training whistle) were played at the same source sound pressure level (sound pressure level) (~86.5 dB re 20 µPa @ 1 m(root mean square)). A high sound pressure level tidal turbine signal was also played at ~94 dB re 20µPa @ 1m (root mean square). Noise was kept to a minimum

during the experimental trials with a resultant median ambient noise of 59.7 dB (95% CIs: 55.7-64.4) re 20µPa (Table S1). All sounds were combined for analysis of auditory stimuli.

Signals were played from an HP Elitebook laptop computer using a speaker (MX Sound, Logitech, Lausanne, Switzerland) located approximately 1 m in front of the animal's head, in line with its longitudinal axis. Transducer calibrations were made using a calibrated mini-DSP UMIK-1 measurement microphone (frequency response: 14Hz – 20kHz ± 1dB) and a laptop computer.

Tactile stimuli consisted of the presence and absence of manual stimulation of either the right or left mystacial and supraorbital vibrissae by gently stroking the whiskers.

Experimental Procedure

Approximately 10-15 min before sensory stimulus experiments, each seal was sedated using a combination of midazolam (Hypnovel, Roche Products Ltd, UK; 5 mg ml^{-1} solution, 0.03 ml kg^{-1} IM) and ketamine (Ketaset, Zoetis, UK 100 mg ml^{-1} solution, 0.01 ml kg^{-1} IV). The seals were then moved to a table in a relatively quiet and evenly lit indoor lab. A respiratory band ('FLOW', Sweetzpot, Oslo, Norway) was placed around the chest to measure respiratory activity, allowing respiratory activity signals to be filtered from the NIRS data. The neoprene headcap was fitted on the seals head ensuring that optodes and detectors were located on the exposed skin. The signal on each channel was checked to ensure continuous cardiac pulsation were present in real-time raw data relay from the fNIRS instrument to a PC, before proceeding with experimental exposures.

The experiments consisted of three epochs (one for each sensory stimulus), each consisting of 8-10 blocks of stimulus presentation (Fig. S2). Each block was 15 s in duration and was followed by 15 s of stimulus-absence. Each epoch was preceded and followed by a 30s period without stimulus. Epoch order was randomised and the order of the sounds presented and the vibrissal assemblage stimulated were randomised within epochs. The presentation of instructions for manual stimulation (visual and tactile stimulation) and presentation of auditory stimulation was controlled using E-Prime 3.0, which also time-stamped each stimulus presentation to the fNIRS control software, Oxysoft (Version 3.2.51.2, Artinis Medical Systems BV, Einsteinweg, The Netherlands). Timings associated with E-Prime, Oxysoft, and the respiratory band were synchronised prior to each experiment. Each seal was exposed to the experimental procedure twice. Each experimental procedure was separated by six (four seals) or seven (one seal) days. This experimental procedure was a balance between assessing as

many stimuli as possible with the minimum amount of stimulus blocks expected to observe a haemodynamic response, whilst minimizing animal handling time.

Analysis of functional near-infrared spectroscopy

To extract the haemodynamic response to evoked neuronal activation, we first manually reviewed trials and removed those that showed large-movement artefacts, sparse respiration events, and detector saturation as determined by the fluctuation magnitude, rate of change and presence of vital signals like heart rate oscillations. For further functional analysis, the NIRS Brain AnalyzIR toolbox [33] was employed, in MATLAB (The MathWorks Inc., Natick, MA, USA). Firstly, a low pass filter was applied to the data to reduce remaining signal noise from motion artefacts. Then, secondly, all data were trimmed to 30 seconds before the first stimulus to 30 seconds after the last stimulus. Thirdly, given the NIRS device had 20 channels across the probe, which equates to 40 measured time traces per animal per condition, processing the resultant 1160 time traces were computationally expensive; we therefore down-sampled the data from 10 to 5 Hz to increase the processing efficiency. However, it is important to highlight that, given the slow nature of a hemodynamic response to neuronal activity, this reduction in sample rate did not affect the capacity to detect cortical activation. Raw intensity values were converted to optical density relative to the average intensity in the first 1% of the data. Remaining motion artefacts resulting in instantaneous intensity changes were removed by applying the temporal derivative distribution repair (TDDR) algorithm [34]. To remove global hemodynamic changes that are caused by systemic influences, such as respiration, heart rate, or blood pressure changes, as well as for further motion artefact reduction, a principle component analysis (PCA) filter was applied. Components of the largest eigenvalues were removed, such that no more than 70% of the variance in each measurement was removed. From here, the modified Beer-Lambert's law was applied, to calculate [ΔHbO], [ΔHbR], and [ΔHbT]. Finally, a bandpass filter with a passband of 0.02 Hz to 0.3 Hz was applied, using a 4^{th} order Butterworth filter.

To extract averaged hemodynamic responses, a time window from 5 s before every stimulation onset to 35 s after the stimulation onset, was extracted for each trial to represent pre-stimulation, stimulation, and post-stimulation data. A two-sample t-test ('ttest2, MATLAB, The MathWorks Inc., Natick, MA, USA) was used to establish the probability of a significant increase in [ΔHbO] or decrease in [ΔHbR] of the signal after stimulation. For this analysis, three seconds of data before the stimulation onset were time-averaged for every stimulation presentation to provide a baseline distribution. Distributions for each three second period

between 5 and 20 seconds after the stimulation onset were then compared to the baseline distribution to identify any statistical differences in pre- and post-stimulus concentrations of [ΔHbO] and [ΔHbR]. A measurement was considered to show a significant change from baseline if any one of the p-values between 5 and 20 seconds after stimulation onset showed $p < 0.05$.

Trials were then averaged per condition (auditory, visual, left tactile, right tactile stimulation) individually for all long-distance channels. In addition, Pearson's correlation ('corrcoef, MATLAB, The MathWorks Inc., Natick, MA, USA) was calculated between [ΔHbO] and [ΔHbR] and used as a condition to distinguish hemodynamic responses, with a negative correlation, from motion, with a positive correlation.

3. Results

The application here of fNIRS successfully measured the hemodynamic response (HR) associated with cortical activation, during stimulation of three sensory pathways (vision, hearing and mechanoreception). Following data filtering 43, 29 and 36 stimulus exposures for visual, auditory and tactile respectively, were analysed for cortical activation detection. In addition to capturing cortical activation, fNIRS also collected high-resolution, continuous data on heart rate and breathing rate.

Localised response to visual stimulation

Channels showing cortical activation during visual stimulation are shown in Fig. 2A. Five channels showed statistically significant group average changes in [HbO], indicative of bilateral cortical activation that occurred predominately in the posterior-medial region of the brain. The group-averaged mean changes in [HbO], [HbR] and [HbT] concentrations in response to a visual stimulus are shown in Fig. 2B. Increase in group-averaged mean (± standard error) [HbO] in active channels were ≤ 0.1 μM. The hemodynamic response was characterised by an overall increase in [HbO] during the period of activation, before declining following stimulus offset.

Fig. 2: (A) Channels displaying statistically significant ($p<0.05$) group average [HbO] changes during visual stimulation are indicated by red dots. The optical array is visualised over the head of a juvenile grey seal to show the anatomical perspective of regional activation. (B) Corresponding group average (lines) and standard error (ribbons) changes in [HbO], [HbR] and [HbT] over 15 s of visual stimulation (shaded grey area) followed by 15 s of no visual stimulation (white area). Bold colours represent a significant ($p<0.05$) changes in [HbO] and where [HbO] and [HbR] were negatively correlated.

Localised response to auditory stimulation

Channels showing cortical activation during auditory stimulation are shown in Fig. 3A. Six channels showed significant group-average changes in [HbO] (Fig. 3A), distributed bilaterally extending anteriorly from the region of activation in posterior of the brain during visual stimulation. The group-averaged mean changes in [HbO] and [HbR] concentrations in response to auditory stimuli are shown in Fig. 3B. Increase in group-averaged mean (± standard error) [HbO] in active channels were ≤ 0.1 μM. HR was characterised by an overall increase in [HbO] following activation, declining during stimulation.

Fig. 3: (A) Channels displaying statistically significant ($p<0.05$) group average [HbO] changes during auditory stimulation are indicated by red dots. The optical array is visualised over the head of a juvenile grey seal to provide anatomical perspective of regional activation. (B) Corresponding group average (lines) and standard error (ribbons) changes in [HbO], [HbR] and [HbT] over 15 s of auditory stimulation (shaded grey area) followed by 15 s of no auditory stimulation (white area). Strong colours represent a significant ($p<0.05$) change in [HbO] and where [HbO] and [HbR] were negatively correlated.

Localised response to tactile stimulation

Channels showing cortical activation during tactile stimulation are shown in Fig. 4A. Four channels showed significant group-average changes in [HbO] (Figs. 4A &5A). Three channels displayed activation during right vibrissal stimulation and one during left vibrissal stimulation. The group averaged mean changes in [HbO] and [HbR] concentrations in response to left vibrissal stimulation are depicted in Figs. 4&5B. Increase in group-averaged mean (±standard error) [HbO] in active channels was ≤ 0.13 μ mol.L^{-1}. HR was characterised by an increase in [HbO] during stimulation, followed by a decline either during stimulation or after stimulus offset.

Fig. 4: (A) Channels displaying statistically significant ($p<0.05$) group average [HbO] changes during **right** vibrissal stimulation are indicated by red dots. The optical array is visualised over the head of a juvenile grey seal to provide anatomical perspective of regional activation. (B) Corresponding group average (lines) and standard error (ribbons) changes in [HbO], [HbR] and [HbT] over 15 s of right vibrissal stimulation (shaded grey area) followed by 15 s of no left vibrissal stimulation (white area). Strong colours represent a significant ($p<0.05$) change in [HbO] and where [HbO] and [HbR] were negatively correlated.

Fig. 5: (A) Channels displaying statistically significant ($p<0.05$) group average [HbO] changes during **left** vibrissal stimulation are indicated by red dots. The optical array is visualised over the head of a

juvenile grey seal to provide anatomical perspective of regional activation. (B) Corresponding group average (lines) and standard error (ribbons) changes in [HbO], [HbR] and [HbT] over 15 s of left vibrissal stimulation (shaded grey area) followed by 15 s of no right vibrissal stimulation (white area). Strong colours represent a significant ($p<0.05$) change in [HbO] and where [HbO] and [HbR] were negatively correlated.

Systemic physiological signals

The hemodynamic consequences of cardiac function and respiration produced clear patterns in the raw fNIRS signals (Fig. 6). Blood volume changes with each cardiac cycle were visible as a cardiac waveform, with greater prominence in [ΔHbO] than [ΔHbR], providing a direct measure of heart rate. As shown in Fig. 6A, heart rate is apparent as clear peaks and troughs in the [ΔHbO] trace. As heart rate in a seal decreased, waveform peak (systolic peak) height increased, indicative of increasing blood pressure (Fig. 6D). Respiration events, which occurred sporadically (approximately every 40-60 s), resulted in significant oscillations in both [ΔHbO] and [ΔHbR] (Fig. 6A). Rapid, deep inspiration (positive peaks in Fig. 6B) caused a rapid increase in [ΔHbO] and a moderate decrease in [ΔHbR] which effectively masked the cardiac waveform. At the end of inspiration, and before breath-holding, animals contracted the thorax (Fig. 6B) which was maintained throughout the remainder of the breath-hold period. Coincident with this thoracic contraction was pronounced bradycardia (as seen in Fig. 6A in the time-series immediately before the black box – where frequency and height of cardiac pulsations are lower), with an increase in [ΔHbO] and a decrease in [ΔHbR]. Seconds after the onset of bradycardia, [ΔHbO] decreased, [ΔHbR] increased, and heart rate increased to a steady rate. On release of the breath-hold, expiration resulted in a rapid decrease in [ΔHbO] and an increase in [ΔHbR].

Fig. 6: (A) Example of the raw [HbO] (red line), [HbR] (blue line) and [HbT] (green line) traces from a seal during the study, showing pulsatile cardiac waveform (for black box see C) and dynamics associated with respiration. (B) Signal from the respiration band where magnitude is directly correlated to chest movement. (C) Cardiac pulsation in [HbO] magnified from the black box in A. (D) Cardiac pulsation of ΔHbT in a grey seal. Colour encodes the underlying heart rate (beats per minute), beginning at diastolic minima at 0 sec and ending at the next diastolic minima, revealing increasing pulse magnitude with lowering heart rates.

4. Discussion

The results presented here demonstrate that cortical hemodynamic alterations in response to sensory stimuli, can be measured with fNIRS in a grey seal. Further, the hemodynamic responses to each stimulus type can be localized and distinguished topographically. These results, together with simultaneous measurement of systemic cardiovascular changes (i.e. heart rate and breathing events), show that fNIRS has the potential to be an important tool for measuring sensory processing and physiological responses of free-ranging animals.

Haemodynamic Response shape

The shape of the haemodynamic response (HR) in seals, for visual, acoustic and tactile stimulation (Figs. 2,3,4 & 5), was comparable to the HR in humans in the dynamics of both [HbO] and [HbR] but was lower in magnitude. The HR in humans is ~1.0 μM [22], while HR here in seals was ≤ 0.1 μM. Therefore, existing fNIRS data-processing protocols (and presumably fMRI) for humans can effectively capture visual, auditory, and tactile sensory brain activation in seals.

Visual stimulation

The visual cortex of almost all mammals is located in the posterior region of the cerebral cortex [18]. Results from the current study showed bilateral regional activation during visual stimulation also occurred in the posterior region of the brain (Fig. 6); this suggests that regional cortical activation in grey seals is consistent with that of other Carnivora, including the domestic dog (*Canis familiaris*) [35-37].

It also confirms predictions of the location of the primary visual cortex of northern elephant seals (*Mirounga angustirostris*) [38] and harp seals (*Pagophilus groenlandicus)* [39] from histological and cytoarchitectural markers on brain samples. These previous studies [38,39] predicted the primary visual cortex to overlap with the arrangement of the four most-posterior and medial channels in Fig. 2A. The posterior medial topographical organisation of the seal visual cortex is also in agreement with visual evoked responses measured in Weddell seals (*Leptonychotes weddellii*) [40].

It is important to highlight that, during visual stimulation in the current study, seals contracted their pupil and directed the pupil towards the light source which would involve motor cortex function. The observed activation that occurred rostral to the visual cortex could therefore be related to motor-cortex activation [41]. Previous work on harbour seals showing that cortical activation can be associated with the motor cortex [42] is also consistent with the rostral topographical activation during visual stimulation in the present study.

Auditory stimulation

The auditory cortex of most mammals is located caudal, ventral, or ventrocaudal to the Sylvian fissure [18]. The lateral arrangement of the auditory cortex in mammals is most often in close proximity to the posterior visual cortex [18]. Other carnivores also display auditory activation ventral to the supra-Sylvian sulcus [43-44]. However, cortical activation during auditory stimulation in harbour seals has been reported more ventrally [45]. Cortical responses to auditory stimulation in the current study showed hemodynamic responses, particularly in the three anteriorly active channels, that are consistent with topographical organisation of the auditory cortex reported by Alderson et al. [45]. Activation to auditory stimulation extended posteriorly into the presumed visual cortex; this may have been a consequence of the seals attempting to visually locate the sound source during playbacks.

Tactile stimulation

Location of the somatosensory cortex appears variable across mammals [18]. However, in most cases, the primary somatosensory cortex is located dorsorostrally to the auditory cortex, and the secondary somatosensory cortex is located in close proximity and rostral to the auditory cortex [18]. In the current study, vibrissal stimulation resulted in predominantly contralateral activation of the cortex and is consistent with previous measurements in northern fur seals (*Callorhinus ursinus*) [46] and other carnivores, such as dogs [18].

During right vibrissal stimulation there was activation predominantly in the right cortex, with a topographical organisation consistent with Ladygina et al. [46]. There was additional activation frontal activation in the left cortex. During left vibrissal stimulation there was a single channel showing activation in the left cortex. The channel showing activation, while contralateral to the side of vibrissal stimulation, was caudal to the expected region of activation. There was, however, non-significant hemodynamic responses in the channel anterior to the significant activation, that would be consistent with right vibrissal stimulation and Ladygina et al. [46].

Physiological monitoring

As we have demonstrated, the changes of [HbO] and [HbR] concentrations measured by fNIRS that allow cortical activation to be detected, also contain a series of important systemic physiological signals such as respiration and cardiovascular function. While physiological signals like heartbeats and respiration tended to show a high signal to noise ratio in NIRS data, for functional imaging these signals are considered artefacts due to their relatively high signal

strength in comparison to functional activation. In humans, where heart rate and respiration are relatively constant in frequency, a frequency-based filter can be used to remove these influences. In seals, the respiration events are intermittent, and heart rate and cerebral blood volume are modulated by respiration; this makes the removal of physiological signals uniquely challenging. For human fNIRS data, numerous methods exist to remove such physiological artefacts from the signal [47,48]. Some of these methods, including general linear models [49], will benefit from the establishment of a species-specific hemodynamic response function (HRF), which is the mathematical description of the relationship between neuronal activation and hemodynamic response or even the shape and duration of the hemodynamic response itself. Although respiration induced the greatest magnitude of physiological contamination, it is important to highlight that seals in the wild spend approximately 80% of their time underwater [50]; the contamination due to respiration observed in the current study is, therefore, likely to be significantly less in wild seals.

Measuring heart rate through haemoglobin concentration fluctuations also provides information on cardiac waveform, which can provide information such as proxies for changes in blood pressure and potentially proxies for changes in intracranial pressure dynamics [51]. Further, analysis of both [HbO] and [HbR] cardiac waveforms can be used to calculate percentage arterial blood oxygen saturation [52] as recently employed to estimate SpO_2 in deep freediving humans [53]. Changes in [HbO] and [HbR] also provides measures of relative blood volume and tissue-specific blood oxygenation [21]. Finally, as a result of blood pressure changes due to intrathoracic pressure variation engendered by respiratory mechanics similar to the four stages of a Valsalva manoeuvre, [HbO] and [HbR] fluctuations with each exhalation, inhalation and apnea can be used to identify individual breaths, as confirmed through the respiratory band data in the current study.

fNIRS in wild animals

This study represents an important first step in developing a biologging tool to measure sensory biology, through cortical activation in wild animals using non-invasive, wearable technology. Measuring sensory-specific regional activation with fNIRS provides a fundamental basis for understanding behavioural decision-making and behavioural interactions (such as locating prey or avoiding predators). Currently, our understanding of how wild animals interpret environmental stimuli is largely hypothetical. We have demonstrated that fNIRS can detect patterns of hemodynamic change associated with cortical activation by sensory stimuli in seals. The topographical organization of cortical regions associated with visual, auditory, and tactile

processing can be differentiated, although some overlap between regional activation does exist. This should allow perception through these three senses to be explored simultaneously and measure their relative importance under different ecological scenarios, such as foraging or predator avoidance.

From an applied perspective, measuring patterns of sensory activation with fNIRS may also offer important new perspectives in studies of the effects of potentially distracting or harmful stimuli from anthropogenic activities. For example, underwater sound from offshore industrial activities has been shown to elicit behavioural responses leading to avoidance in seals [6,54]. However, responses by animals appear to be highly context-specific [55] such that behavioural responses (or lack thereof) may be mediated by attentional factors, such as whether an animal is already engaged in an important activity such as foraging, which involves other senses that affect sound detection or decisions in how they respond. fNIRS could potentially allow an understanding of the underlying mechanisms and priority stimuli that contribute to decision making, particularly when behavioural responses are potentially costly.

Development considerations for an animal-borne fNIRS logger

The integration of fNIRS cortical activation data and the associated physiological data into existing behavioural and environmental data logging platforms [7,54] could provide a powerful suite of instantaneous and continuous measures of responses to external stimuli as animals interact with their environment in the wild. However, the current study was carried out on animals under controlled conditions, and there are a series of additional translational steps required before free-ranging animal studies are feasible.

1. In the current study, senses were stimulated independently from others, whereas in the wild it is unlikely that animals will rely on only one sense at any one-time during events such as prey capture. Therefore, an important progression would be to conduct experiments that present combinations of single-sensory and multi-sensory stimulation to assess the capacity of fNIRS and to identify which senses are in use and potential time-dependent sensory dominance.
2. The results presented here were to a series of playbacks and sensory stimulations in air. For aquatic species such as seals, it would be useful to repeat these underwater to confirm that the patterns of activation are consistent across mediums.
3. Measuring NIRS signals in mobile subjects is significantly more challenging due to the influence of factors such as motion artefacts [56]. Therefore, efforts to study mobile

animals in managed or controlled conditions would be an advisable next step. Reducing/managing impact of motion artefacts could be addressed either mechanically, through appropriate optode/receiver attachment, or computationally, through signal processing. In humans, motion artefacts are easily generated through head movements that cause decoupling between optode/detectors and the scalp. The use of headcaps in human fNIRS research, that cradle and locate the optode/detectors could be improved upon in animal research to generate more robust, continual contact between hardware and the scalp, that is less sensitive to body movement. Alternatively, the use of adhesives for instrument attachment is routine in animals such as seals and are likely to reduce motion artefacts issues that impact human fNIRS research by providing more reliable hardware/skin contact. Furthermore, a range of available fNIRS motion artefact detection and correction approaches could be applied here [56]. These approaches, some of which could utilise existing animal-borne technology such as accelerometers [57], could be helpful for recovering usable fNIRS signals in mobile animals.

4. Whilst the current study demonstrates the efficacy and utility of fNIRS in a single species, there are important considerations for its future development and application across species. For example, from a neuroimaging perspective, substantial work has been conducted on humans to facilitate translation of signals derived from the scalp to the brain. However, the accuracy of topographical projections of cortical activation signals is currently relatively limited for new species. To ensure fNIRS can be applied to new animal models, accurate topographical projections of animals with fundamentally different skull shapes, skull thicknesses, extracranial anatomical differences, and gross physiological differences would likely be required. This is required to ensure that optode array placements in relation to skull morphological features can be standardised and allow meaningful comparisons between species, and age-classes. Collaboration with anatomists and neuroanatomists may be of great importance in the future if independent studies with fNIRS are to be comparable and more accurate. Alternatively, neuroanatomical tools such as MRI (where feasible) would potentially help to understand the regions of the brain interrogated with the fNIRS optical path.
5. Another important precursor to using fNIRS in any new species is the accurate measurement of the optical properties of different tissues (skin, muscle, fat, skull, blood, brain) as these may affect the penetration of existing wavelengths in commercial fNIRS systems and may inform optimal alternate wavelengths required. Coupling

optical property measurements with 3D Monte Carlo simulations [58] would provide more accurate estimation of where in the brain the activation is being measured. In the current study, we used commercially available wavelengths suitable for humans, because seal haemoglobin has similar optical properties to humans [59], there is a short distance from scalp to brain (< 1.5 cm – typically less than a human), and fNIRS has been successfully used on seals to measure blood volume in brain and blubber [21]. However, for species without this information, the absorption and scattering coefficients should be measured, and the dynamics of optical propagation estimated.

6. In terms of the physical deployment of an fNIRS logger on an animal, it is important that this is not only robust but does not unduly influence the behaviour or energetics of the animal [60]. Appropriate ruggedisation/marinization while maintaining optical-integrity and appropriate attachment protocols is therefore required to allow fNIRS to be used on wild animals. Initial work on seals [21] and deep-diving humans [53], although restricted to single-channel systems, has shown that this is readily achievable even for extreme environmental conditions.

5. Conclusion

We have shown fNIRS can be used to measure sensory activation, along with simultaneous measurement of systemic cardiovascular changes (i.e. heart rate and breathing events) in seals, and demonstrate that its powerful applications in human biomedical and cognitive research could translate to free-ranging wild animal research. The capacity of fNIRS to simultaneously capture cortical activation and systemic physiological responses in a non-invasive, wearable instrument may facilitate free-ranging measurements. Together with data from existing animal-borne behavioural and environmental data logging systems, such data could provide key information to understanding sensory perception, behavioural responses, and decision-making in wild animals.

References

1. Thompson D, Fedak MA. 2001. How long should a dive last? A simple model of foraging decisions by breath-hold divers in a patchy environment. Anim. Behav. 61 (2), 287-296.
2. Sparling CE, Georges J-Y, Gallon SL, Fedak M, Thompson D. 2007. How long does a dive last? Foraging decisions by breath-hold divers in a patchy environment: a test of a simple model. Anim. Behav. 74, 207-218. https://doi.org/10.1016/j.anbehav.2006.06.022
3. Hanke W, Dehnhardt G. 2013. Sensory biology of aquatic mammals. J. Comp. Physiol. A., 199, 417. https://doi.org/10.1007/s00359-013-0823-9
4. Cox TM, Ragen TJ, Read AJ, Vos E, Baird RW, Balcomb K, Barlow J, Caldwell J, Cranford T, Crum L, D'Amico A, D'Spain G, Fernandez A, Finneran JJ, Gentry RL,

Gerth W, Gulland F, Hildebrand J, Houser D, Huller T, Jepson PD, Ketten DR, MacLeod CD, Miller P, Moore S, Mountain DC, Palka D, Ponganis P, Rommel S, Rowles TK, Taylor B, Tyack PL, Wartzok D, Gisiner RC, Mead JG, Benner L. 2006. Understanding the impacts of anthropogenic sound on beaked whales. J. Cetac. Res. Manage. 7*,* 177-187.

5. Slabbekoorn H, Bouton N, Van Opzeeland I, Coers A, ten Cate C, Popper AN. 2010. A noisy spring: the impact of globally rising underwater sound levels on fish. Trends Ecol. Evol. 27(7), 419-427.
6. Hastie GD, Russell DJF, Lepper P, Elliott J, Wilson B, Benjamins S, Thompson D. 2017. Harbour seals avoid tidal turbine noise: Implications for collision risk. J. Appl. Ecol. 55(2), 684-693.
7. Mikkelsen L, Johnson M, Wisniewska DM, van Neer A, Siebert U, Madsen T, Teilmann J. 2019. Long-term sound and movement recording tags to study natural behaviour and reaction to ship noise of seals. Ecol. Evol. 9(5), 2588-2601.
8. Searby A, Jouventin P. 2003. Mother-lamb acoustic recognition in sheep: a frequency coding. Proc. R. Soc. Lond. B. *270*, 1765–1771
9. Kendrick KM. 1994. Neurobiological correlates of visual and olfactory recognition in sheep. Behav. Process. 33 (1–2), 89-111.
10. Hanke FD, Dehnhardt G, Schaeffel F, Hanke W. 2006. Corneal topography, refractive state, and accommodation in harbour seals (*Phoca vitulina*). Vis. Res. 46*,* 837–847.
11. Dykes RW. 1975. Afferent fibres from mystacial vibrissae of cats and seals. J. Neurophysiol. 38(3), 650-662.
12. Hanke FD, Hanke W, Scholtyssek C, Dahnhardt G. 2009. Basic mechanisms in pinniped vision. Exp. Brain Res. 199*,* 299. https://doi.org/10.1007/s00221-009-1793-6
13. Reichmuth C, Holt MM, Mulsow J, Sills JM, Southall BL. 2013. Comparative assessment of amphibious hearing in pinnipeds. J. Comp. Physiol. A. 199, 491. https://doi.org/10.1007/s00359-013-0813-y
14. Wieskotten S, Mauck B, Miersch L, Dehnhardt G, Hanke W. 2011. Hydrodynamic discrimination of wakes caused by objects of different size and shape in a harbour seal (*Phoca vitulina*). J. Exp. Biol. 214, 1922-1930.
15. Gläser N, Wieskotten S, Otter C, Dehnhardt G, Hanke W. 2011. Hydrodynamic trail following in a California sea lion (Zalophus californianus). J. Comp. Physiol. A. 197, 141-151.
16. Vacquié-Garcia J, Mallefet J, Ballieul F, Picard B, Guinet C. 2017. Marine bioluminescence: Measurement by a classical light sensor and related foraging behaviour of a deep diving predator. J. Photochem. Photobiol. B. 93(5), 1312-1319. https://doi.org/10.1111/php.12776
17. Durlach NI, Mason CR, Kidd G, Arbogast TL, Colburn HS, Shinn-Cunningham BG. 2003. Note on informational masking (L). J. Acout. Soc. Am. 113, 2984. https://doi.org/10.1121/1.1570435
18. Johnson JI. 1990. Comparative development of somatic sensory cortex. In: Jones E.G., Peters A. (eds) Cerebral Cortex. Cerebral Cortex, vol 8B. Springer, Boston, MA. http://doi-org-443.webvpn.fjmu.edu.cn/10.1007/978-1-4615-3824-0_6
19. Strangman G, Culver JP, Thompson JH, Boas DA. 2002. A quantitative comparison of simultaneous BOLD fMRI and NIRS recordings during functional brain activation. NeuroImage, 17, 719-731. doi:10.1006/nimg.2002.1227
20. Ferrari M, Quaresima V. 2012. A brief review on the history of human functional near-infrared spectroscopy (fNIRS) development and fields of application. Neuroimage, 63(2), 921–935. pmid:22510258

21. McKnight JC, Bennett KA, Bronkhorst M, Russell DJF, Balfour S, Milne R, Bivins M, Moss SEW, Colier W, Hall AJ, Thompson D. 2019. Shining new light on mammalian diving physiology using wearable near-infrared spectroscopy. PLoS Biol. 17(6), e3000306
22. Boas DA, Gaudette T, Strangman G, Cheng X, Marota JJA, Mandeville JB. 2001. The accuracy of Near Inreared Spectroscopy and Imaging during Focal Changes in Cerebral Hemodynamics. NeuroImage, 13, 76-90. dos:10.1006/nimg.2000.0674
23. Pinti P, Scholkmann F, Hamilton A, Burgess P. Tachtsidis I. 2019. Current status and issues regarding pre-processing of fNIRS neuroimaging data: An investigation of diverse signal filtering methods within a General Linear Model framework. Front. Hum. Neurosci. 12. Doi:10.3389/fnhum.2018.00505
24. Butler PJ, Green GA, Boyd IL, Speakman JR. 2004. Measuring metabolic rate in the field: the pros and cons of the doubly labelled water and heart rate methods. Funct. Ecol. 18, 163-183.
25. Williams TM, Blackwell SB, Richter B, Sinding M-HS, Heide-Jørgensen MP. 2017. Paradoxical escape responses by narwhals (Monodon monoceros). Science. 358, 1321-1331.
26. Gygax L, Reefman N, Pilheden T, Scholkmann F, Keeling L. 2015. Dog behaviour but not frontal reaction changes in repeated positive interactions with a human: A non-invasive pilot study using functional near-infrared spectroscopy (fNIRS). Behav. Brain Res. 281*,* 172-176. https://doi.org/10.1016/j.bbr.2014.11.044
27. Kawaguchi H, Higo N, Kato J, Matsuda K, Yamada T. 2017. Functional near infrared spectroscopy for awake monkey to accelerate neurorehabilitation study. Proc. SPIE 10051, Neural Imaging and Sensing, 1005117 (8 February 2017); https://doi.org/10.1117/12.2250080
28. Chincarini M, Qiu L, Spinelli L, Torricelli A, Minero M, Dalla Costa E, Mariscoli M, Ferri N, Giammarci M, Vignola F. 2019. Evaluation of sheep anticipatory response to a food reward by means of functional near-infrared spectroscopy. Animals. 9(1), 11. pmid:30597931
29. Kastelein RA, Hoek L, Wensveen PJ, Terhune JM. 2010. The effect of signal duration on the underwater hearing thresholds of two harbor seals (*Phoca vitulina*) for single tonal signals between 0.2 and 40 kHz. J. Acoust. Soc. Am. 127, 1135-1145.
30. Hastie GD, Merchant ND, Götz T, Russell DJF, Thompson P, Janik VM. 2019. Effects of impulsive noise on marine mammals: investigating range-dependent risk. Ecol. Appl. 29(5), e01906
31. Heindenreich B. 2007. An introduction to positive reinforcement training and its benefits. J. Exot. Pet Med. 16(1*),* 19-23.
32. Sassaroli A, Fantini S. 2004. Comment on the modified Beer-Lambert law for scattering media. Phys. Med. Biol. 49 (14), N255–N257.
33. Santosa H, Zhai X, Fishburn F, Huppert T. 2018. The NIRS Brain AnalyzIR toolbox. Algorithms. 11, doi:10.3390/A11050073
34. Fishburn FA, Ludlum RS, Vaidya CJ, Medvedev AV. 2019. Temporal Derivative Distribution Repair (TDDR): A motion correction method for fNIRS. Neuroimage. 184, 171–179. doi:10.1016/j.neuroimage.2018.09.025
35. Dilks DD, Cook P, Weiller SK, Berns HP, Spivak M, Berns GS. 2015. Awake fMRI reveals a specialized region in dog temporal cortex for face processing. PeerJ. 3, e1115 https://doi.org/10.7717/peerj.1115
36. Berns GS, Brooks AM, Spivak M, Levy K. 2017. Functional MRI in awake dogs predicts suitability for assistance work. Sci. Reports. 7, 43704

37. Thompkins AM, Ramaiahgari B, Zhao S, Gotoor SSR, Waggoner TS, Deshpande G, Katz JS. 2018. Separate brain areas for processing human and dog faces as revealed by awake fMRI in dogs (*Canis familiaris*). Learn Behav. 46**,** 561–573, https://doi.org/10.3758/s13420-018-0352-z
38. Turner EC, Sawyer EK, Kaas JH. 2017. Optic nerve, superior colliculus, visual thalamus, and primary visual cortex of the northern elephant seal (*Mirounga angustirostris*) and California sea lion (*Zalophus californianus*). J Comp Neurol. 525, 2109– 2132. https://doi.org/10.1002/cne.24188
39. Walloe S, Eriksen N, Dabelsteen T, Pakkenberg B. 2010. A neurological comparative study of the harp seal (Pagophilus groenlandicus) and harbor porpoise (Phocoena phocoena) brain. Anat. Rec. 293, 2129–2135.
40. Gruenau SP, Shurley JT. 1976. Visual evoked response (VER) changes during maturation in the Weddell seal. J. Dev. Physiol. 9, 477-493.
41. Pierrot-Deseilligny C, Milea D, Muri RM. 2004. Eye movement control by the cerebral cortex. Curr. Opin. Neurol. 17(1), 17-25.
42. Langworthy OR, Hesser F, Kolb LC. 1938. A physiological study of the cerebral cortex of the hair seal (Phona vitulina). J. Comp. Neurol. 69(3), 351-369.
43. Brown TA, Joanisse MA, Gati JS, Hughes SM, Nixon PL, Menon RV, Lomber SG. 2013. Characterization of the blood-oxygen level-dependant (BOLD) response in cat auditory cortex using high-field fMRI. NeuroImage, 64, 458-465.
44. Gábor A, Gácsi M, Szabó D, Miklósi Á, Kubinyi E, Andics A. 2020. Multilevel fMRI adaptation for spokes word processing in the awake dog brain. Sci. Reps. 10*,* Article number: 11968.
45. Alderson AM, Diamantopoulos E, Downman CBB. 1960. Auditory cortex of the seal (Phoca vitulina). J. Anat. 94(4), 506-511.
46. Ladygina TF, Popov VV, Supin AY. 1985. Topical organization of somatic projections in the fur seal cerebral cortex. Neurophysiol. 17*,* 246-252.
47. Brigadoi S, Ceccherini L, Cutini S, Scarpa F, Scatturin P, Selb J, Gagnon L, Boas DA, Cooper RJ. 2014. Motion artifacts in functional near-infrared spectroscopy: A comparison of motion correction techniques applied to real cognitive data. Neuroimage. 85, 181–191. doi:10.1016/j.neuroimage.2013.04.082
48. Cooper RJ, Selb J, Gagnon L, Phillip D, Schytz HW, Iversen HK, Ashina MA, Boas DA. 2012. A systematic comparison of motion artifact correction techniques for functional near-infrared spectroscopy. Front Neurosci. 6, 1–10. doi:10.3389/fnins.2012.00147
49. Huppert TJ. 2016. Commentary on the statistical properties of noise and its implication on general linear models in functional near-infrared spectroscopy. Neurophotonics. 3, 010401. doi:10.1117/1.nph.3.1.010401
50. Thompson D, Hammond PS, Nicholas KS, Fedak MA. 1991. Movements, diving and foraging behaviour of grey seals (Halichoerus grypus). J. Zool. Lond. 224, 223-232.
51. Ruesch A, Yang J, Schmitt S, Acharya D, Smith MA, Kainerstorfer JM. 2020. Estimating intracranial pressure using pulsatile cerebral blood flow measured with diffuse correlation spectroscopy. Biomed. Opt. Express. 11(3), 1462-1476.
52. Massen J, Colier W, Hopman J, Liem D, de Korte C. 2009. A method to calculate arterial and venous saturation from near infrared spectroscopy. Adv. Exp. Med. Biol. 645*,* 135-140.
53. McKnight JC, Mulder E, Ruesch A, Kairnerstorfer J, Wu J, Hakimi N, Balfour S, Bronkhorst M, Parnett F, Tyack P, Horschig J, Hastie G, Schagatay E. 2020. When the human brain goes diving: Cerebral and Systemic Cardiovascular Responses to Deep, Breath-Hold Diving in Elite Freedivers. *In Review*. Phil. Trans. Proc. Soc. B.
54. Russell DJF, Hastie GD, Thompson D, Janik VM, Hammond PS, Scott-Hayward LAS, Matthiopoulos J, Jones EL, McConnell BJ. 2016. Avoidance of wind farms by harbour seals is limited to pile driving activities. J. Appl. Ecol. 53(6), 1642-1652.

55. Goldbogen JA, Southall BL, DeRuiter SL, Calambokidis J, Friedlaender AS, Hazen EL, Falcone EA, Schorr GS, Douglas A, Moretti DJ, Hyburg C, McKenna MF, Tyack PL. 2013. Blue whales respond to simulated mid-frequency military sonar. Proc. Roy. Soc. B. 280, https://doi.org/10.1098/rspb.2013.0657
56. Brigadoi S, Ceccherini L, Cutini S, Scarpa F, Scatturin P, Selb J, Gagnon L, Boas DA, Cooper RJ. 2014. Motion artefacts in functional near-infrared spectroscopy: A comparison of motion correction techniques applied to real cognitive data. NeuroImage. 85(1),181-191.
57. Virtanen J, Noponen T, Kotilahti K, Virtanen J, Ilmoniemi RJ. 2011. Accelerometer-based method for correcting signal baseline changes caused by motion artifacts in medical near-infrared spectroscopy. J. Biomed. Opt. 16 (8), p. 087005
58. Haeussinger FB, Heinzel S, Hahn T, Schecklmann M, Ehlis A-C, Fallgatter AJ. 2011. Simulation of near-infrared light absorption considering individual head and prefrontal cortex anatomy: Implications for optical neuroimaging. PLoS One. 6(10), E26377.
59. Tift MS, Ponganis PJ, Crocker DE. 2014 Elevated carboxyhemoglobin in a marine mammal, the northern elephant seal. J. Exp. Biol. 217, 1752–1757.
60. Rosen DAS, Gerlinsky CG, Trites AW. 2018. Telemetry tags increase the costs of swimming in northern fur seals, Callorhinus ursinus. Mar. Mam. Sci. 34, 385-402. doi:10.1111/mms.12460

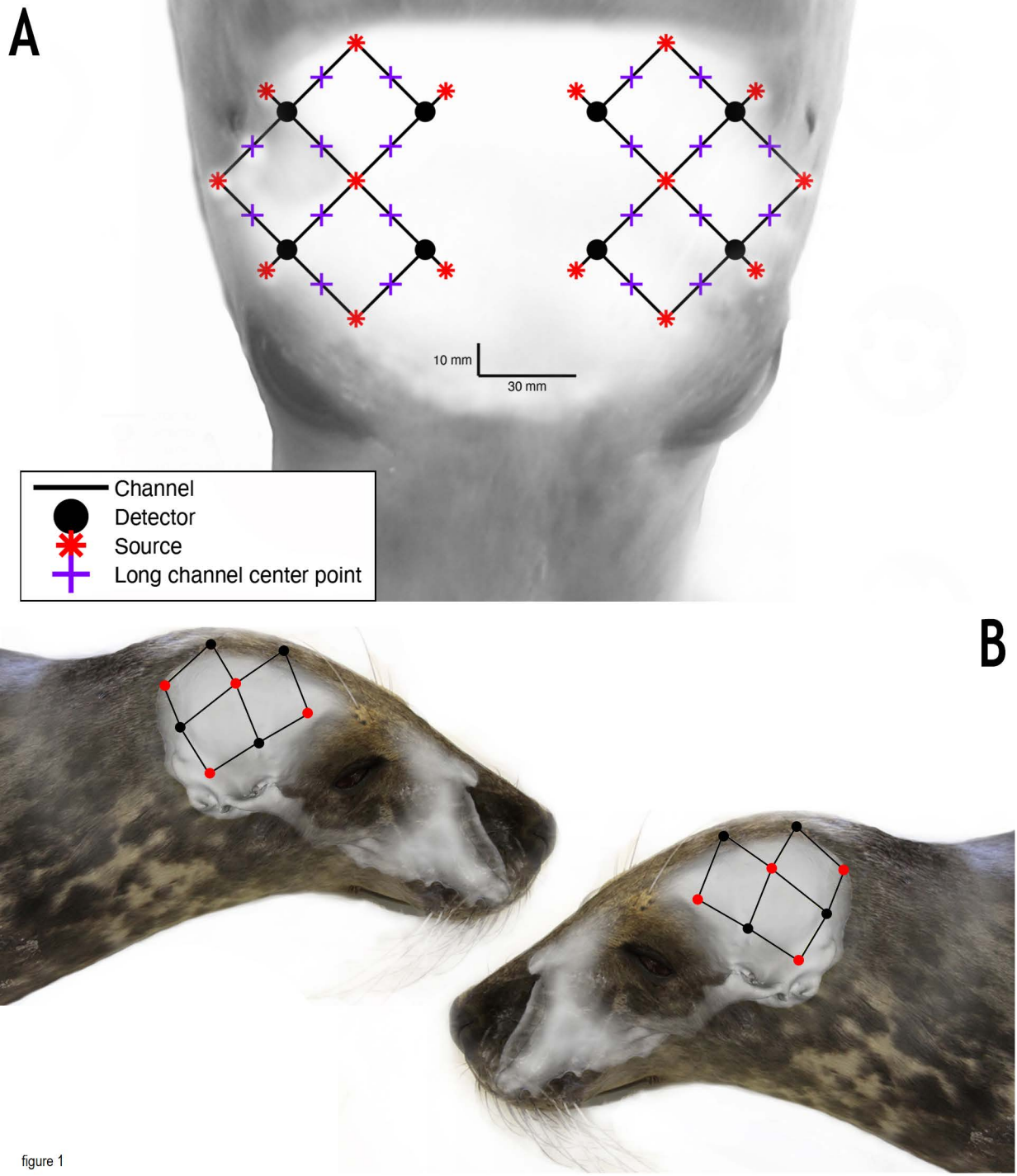
A
10 mm
30 mm
Channel
Detector
Source
Long channel center point
B

figure 1

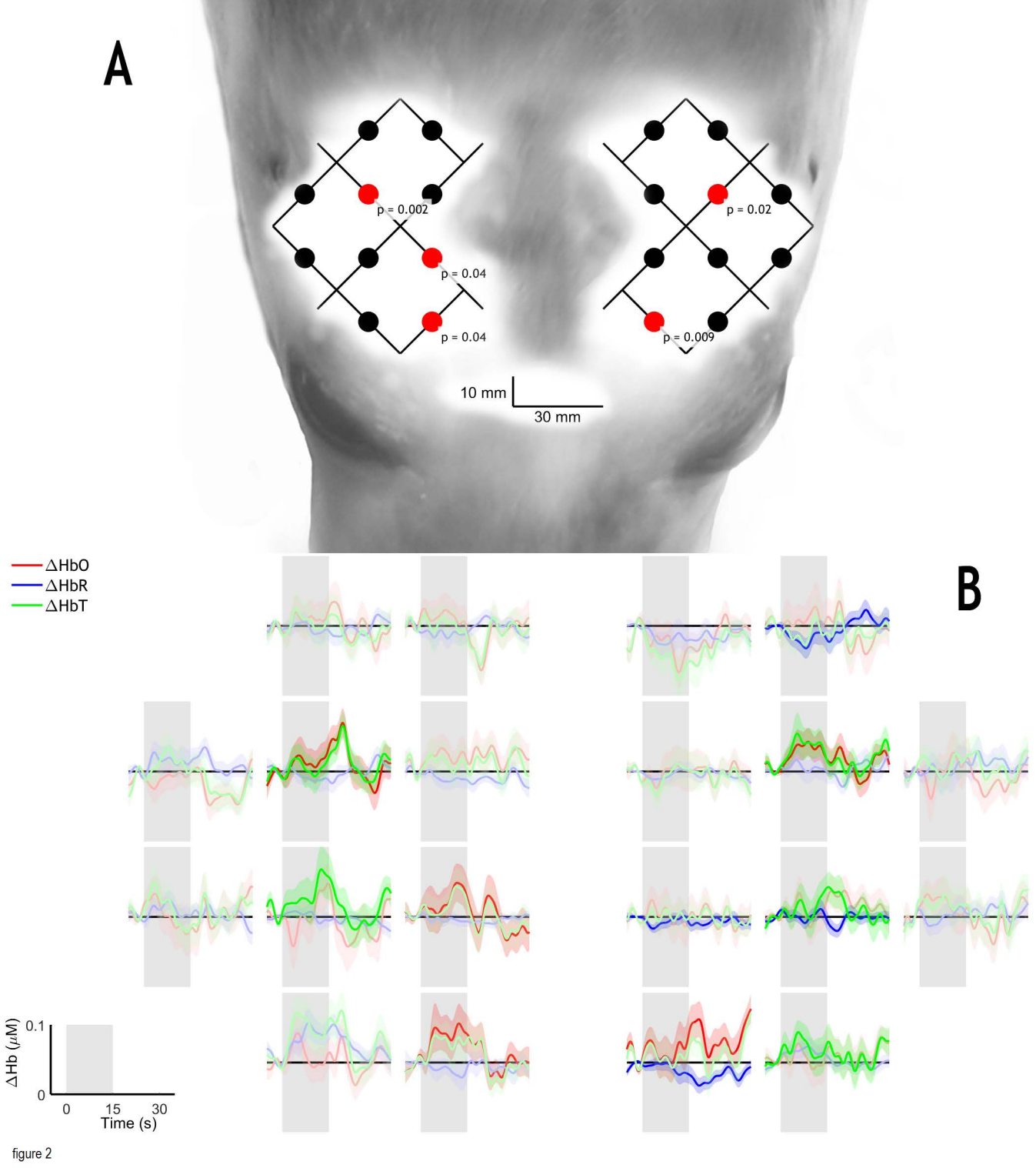
A
p = 0.002
p = 0.04
p = 0.04
p = 0.02
p = 0.009
10 mm
30 mm
ΔHbO
ΔHbR
ΔHbT
B
ΔHb (μM)
0.1
0
0
15
30
Time (s)

figure 2

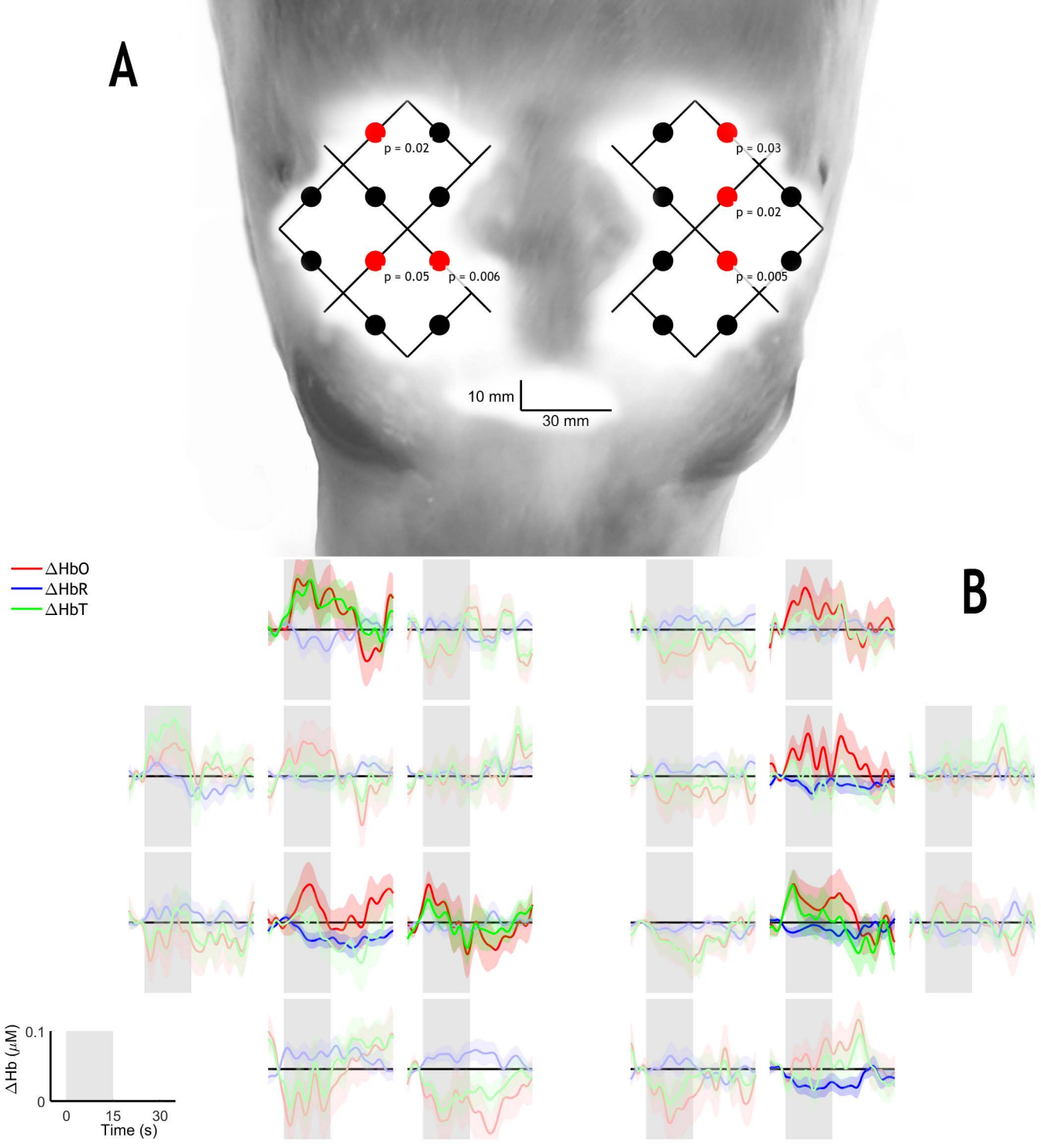
A
p = 0.02
p = 0.05
p = 0.006
p = 0.03
p = 0.02
p = 0.005
10 mm
30 mm
ΔHbO
ΔHbR
ΔHbT
B
ΔHb (μM)
0.1
0
0
15
30
Time (s)

figure 3

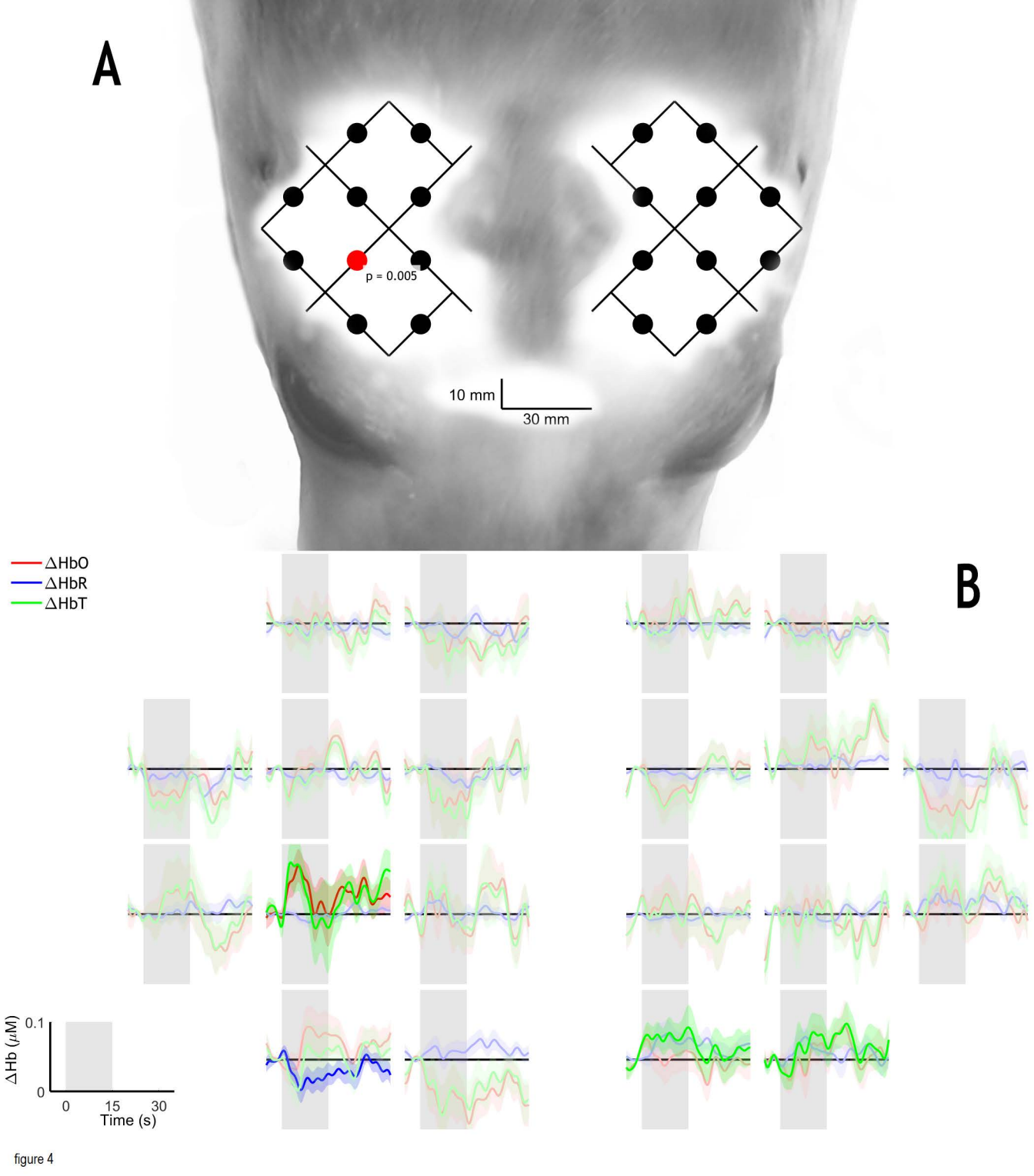

figure 4

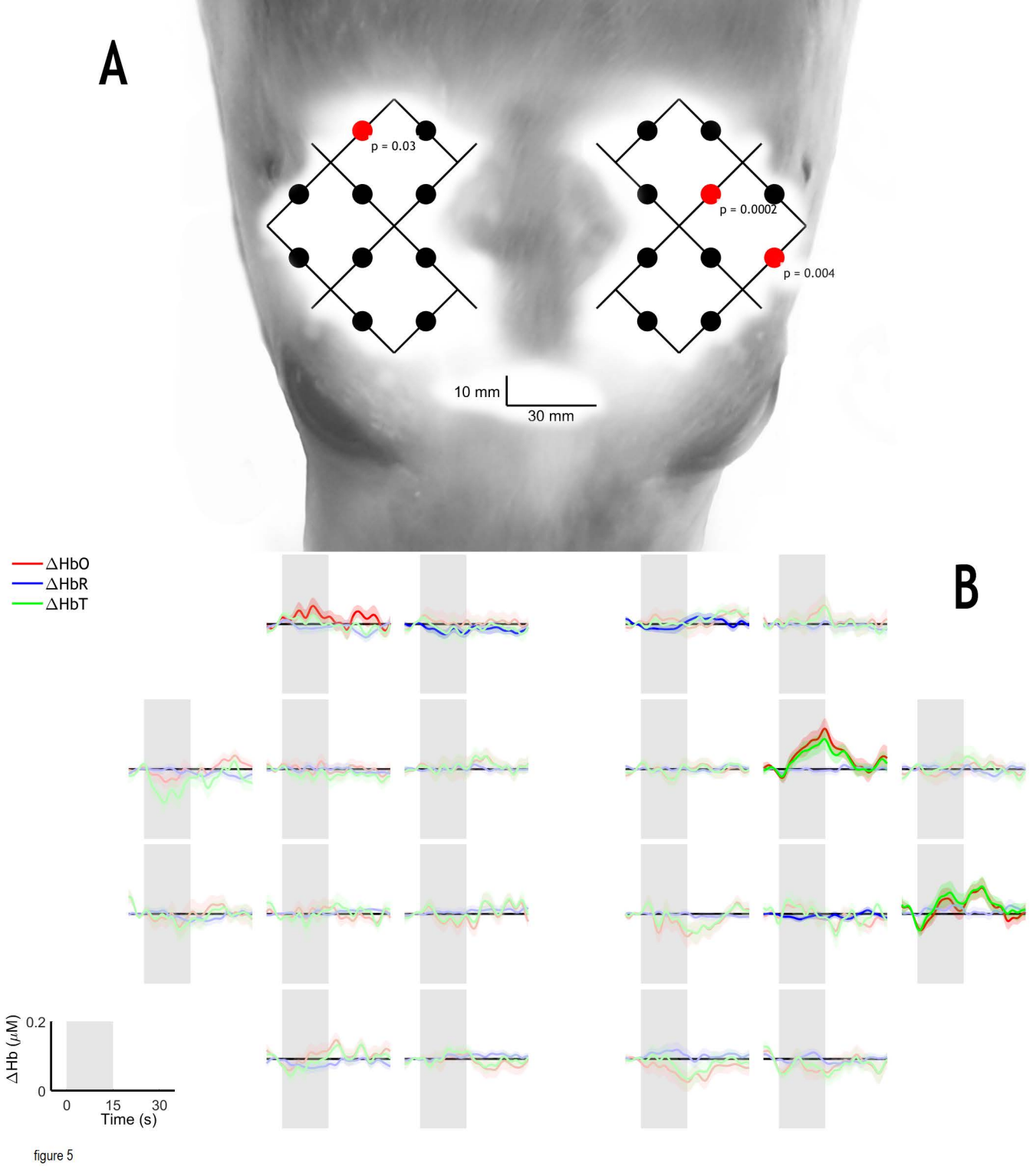
A
p = 0.03
p = 0.0002
p = 0.004
10 mm
30 mm
ΔHbO
ΔHbR
ΔHbT
B
ΔHb (μM)
0.2
0
0
15
30
Time (s)

figure 5

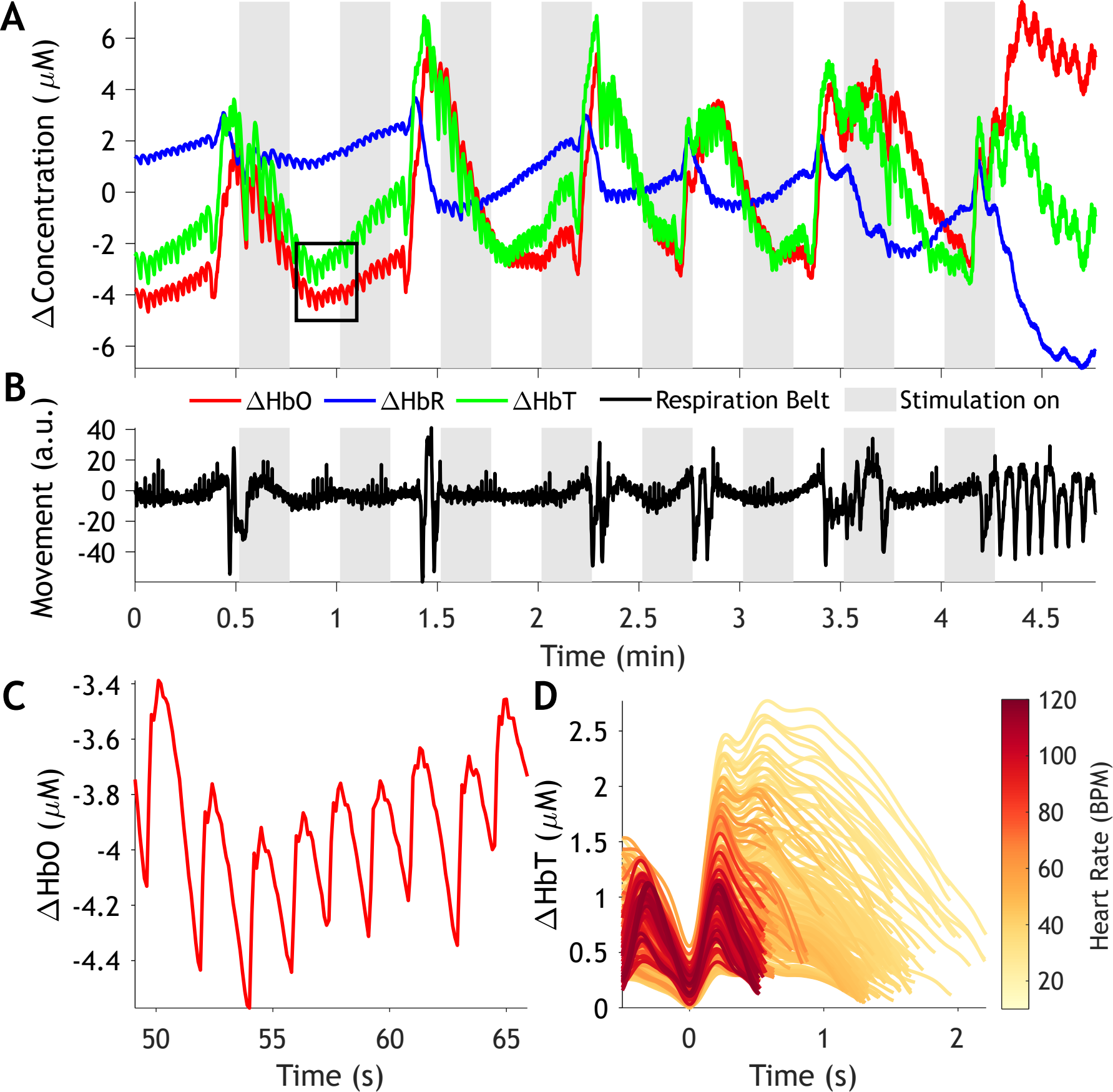
A
ΔConcentration (μM)
6
4
2
0
-2
-4
-6
B
ΔHbO
ΔHbR
ΔHbT
Respiration Belt
Stimulation on
Movement (a.u.)
40
20
0
-20
-40
0
0.5
1
1.5
2
2.5
3
3.5
4
4.5
Time (min)
C
ΔHbO (μM)
-3.4
-3.6
-3.8
-4
-4.2
-4.4
50
55
60
65
Time (s)
D
ΔHbT (μM)
2.5
2
1.5
1
0.5
0
0
1
2
Time (s)
120
100
80
60
40
20
Heart Rate (BPM)